COMPRESSIBILITY EFFECTS IN THE HIGH-SPEED, REACTING SHEAR LAYER

C. Pantano and S. Sarkar
Department of AMES
University of California San Diego
9500 Gilman Dr., La Jolla CA 92093-0411, USA

ABSTRACT

Thermodynamic variables exert a strong influence on the flow field in high-speed combustion. Direct simulation of the shear layer is used to investigate the coupling between thermodynamic fluctuations and the turbulent flow in subsonic-to-supersonic regimes and over a wide range of density ratios. The high-speed effect is parametrized by the convective Mach number, M_c, while density heterogeneity is characterized by the ratio of free-stream densities, $s = \rho_2/\rho_1$. With increasing M_c, a large reduction in thickness growth rate is observed. Analysis and direct simulation is used to offer a mechanism based on the finite speed of pressure fluctuations and consequent temporal decorrelation to explain the reduced growth rate in the high-speed regime. The character of the underlying thermodynamic fluctuations is found to change from the uniform density case to the non-uniform cases. The acoustic mode dominates the former while the entropy mode dominates the latter. An increase of the density fluctuations, with increasing s, is observed while pressure fluctuations decrease.

1 Introduction

Non-premixed combustion in the high-speed regime involves strong coupling between the turbulent flow, thermodynamic variables and chemical species which is poorly understood. The effects on the flow field, in the case of low-speed reacting flows in an open domain, is primarily through changes in the density. In the high-speed regime, both density and pressure changes are potentially important. DNS is a powerful and viable tool to investigate the influence of thermodynamic fluctuations on the turbulent flow and associated scalar mixing. Recent DNS studies of the the non-reacting high-speed shear layer include Vreman *et al.* (1996) while that by Miller *et al.* (1994) considers a simple, one-step exothermic reaction, in addition. The current paper focuses on the effects of high Mach number and of large density variation on the flow and scalar mixing.

At high Mach number, the growth of the turbulent shear layer is substantially reduced. This stabilizing effect is one of the most remarkable features distinguishing compressible turbulence from its incompressible counterpart. Observations of the reduced growth rate at high speeds are numerous. Early experimental evidence is discussed by Bradshaw (1977), and Kline *et al.* (1982) while later experimental and numerical investigations are reviewed by Lele (1994) and Smits & Dussauge (1996).

The convective Mach number, M_c, introduced by Bogdanoff (1983) has become popular as the parameter that determines compressibility effects. Denoting the velocity, density and speed of sound in the high-speed stream by U_1, ρ_1, c_1 and corresponding quantities in the low-speed stream by U_2, ρ_2, c_2 and, assuming equal specific heats, gives $M_c = (U_1 - U_2)/(c_1 + c_2)$. From experimental data, see Figure 1 for example, it is clear that there is a general trend of decreasing thickness growth rate with increasing values of M_c. In the case of high-speed propulsion, there is an additional effect, namely, density changes due to changes in composition and heat release. Therefore, the related question of how the density ratio, $s = \rho_2/\rho_1$, affects the growth rate is of interest.

Identification of the mechanisms responsible for the inhibited shear layer growth at high Mach number is of interest both to gain a fundamental understanding of the problem as well as to derive insights into possible mixing enhancement strategies. DNS studies by Sarkar (1995) of uniformly sheared flow, by Vreman *et al.* (1996) of the plane shear layer, and by Freund *et al.* (1997) of the annular shear layer show that the turbulent production decreases with increasing Mach number. Thus, a reason, based on turbulence energetics, for the reduced thickness of the shear layer is decreased turbulent production. Investigation as to why compressibility reduces

turbulent production is now required. Reduced pressure fluctuations with increasing Mach number has been observed by Vreman *et al.* (1996) in the shear layer, by Sarkar (1996) in the uniformly sheared case, and by Freund *et al.* (1997) in the annular mixing layer and has prompted suggestions that the compressibility effect is linked to pressure fluctuations. However, a complete mechanistic explanation is lacking and is an objective of this work.

There is no systematic study that studies the effect of density ratio on the flow and mixing at high speeds. Therefore, a DNS study is conducted here by varying the density ratio while keeping the Mach number constant. The relative importance of the 'acoustic' mode and the 'entropy' mode in the thermodynamic fluctuations is also obtained.

2 Problem Formulation

The unsteady, three dimensional, compressible Navier-Stokes equations are solved for the temporally-evolving shear layer. The energy equation is written as a pressure equation where viscosity, diffusion, thermal conductivity and the specific heat ratio are constants. The equation of state corresponding to an ideal gas is assumed. A passive scalar is computed along with the flow variables.

2.1 Numerical Scheme

The transport equations are integrated using a 3-4-3 order of accuracy compact Padé scheme in space as described by Lele (1992). The time advancement is performed with a fourth order of accuracy low storage Runge-Kutta scheme as described by Williamson (1980). Periodic boundary conditions in x_1 and x_3 directions are used and 'non-reflective' boundary conditions as studied by Thompson (1987) are imposed in the x_2 direction . A uniform grid is used. In order to avoid spurious numerical instabilities introduced by the boundary conditions in the x_2 direction, the flow variables are filtered every time step using a compact filter described by Lele (1992) of the same accuracy ie; fourth order, as the spatial discretization. Sufficient resolution is used and the filter coefficient chosen as discussed by Lele (1992) to significantly affect only the highest wave numbers. The integration of the scalar variable is performed using a non linear integration scheme. The flux corrected transport scheme as described by Zalesak (1979) is chosen. This scheme guarantees that the passive scalar is kept between its bounds of 0 and 1.

2.2 Initial Conditions

The flow is initialized to a hyperbolic tangent profile for the mean streamwise velocity, $\tilde{u}_1(x_2)$, while all other mean velocity components are set to zero. The upper stream has a velocity, $-\Delta u/2$, and the lower stream has a velocity, $\Delta u/2$. The mean pressure is set to a uniform value p_o. The density in the upper stream ρ_1, and that in the lower stream ρ_2, are specified. The convective Mach number introduced by Bogdanoff (1983) and further studied by Papamoschou & Roshko (1988) is defined in the case of two streams with the same specific heat ratio γ, by $M_c = \Delta u/(c_1 + c_2)$, where c_1 and c_2 are the speeds of sound of each stream. In addition to these mean values, broadband fluctuations are used to accelerate the transition to turbulence. This is achieved by generating a solenoidal random field with an isotropic turbulence spectrum.

Case	M_c	s	L_xxL_yxL_z	N_xxN_yxN_z
A3	0.3	1.0	690x517x345	256x192x128
A7	0.7	1.0	690x517x345	256x192x128
A11	1.1	1.0	690x1142x345	256x384x128
B4	0.7	4.0	690x517x345	256x192x128
B8	0.7	8.0	690x517x345	256x192x128

Table 1. Simulation parameters. L_x, L_y, and L_z denote computational domain lengths measured in terms of initial momentum thickness while N_x, N_y and N_z denote the corresponding number of grid points.

2.3 Simulation parameters

Two series of simulations are conducted. The parameters of series A are chosen to analyze the effects of M_c (compressibility) and those of series B to analyze the effect of variable density for a fixed $M_c = 0.7$ case. The density ratio is defined as $s = \rho_2/\rho_1$. The average density, $\rho_o = (\rho_1 + \rho_2)/2 = 0.7$, is fixed in all the simulations. In series A, the mean density is uniform, while, in series B, the mean density profile is initialized to a hyperbolic tangent profile. The nondimensional parameters in the governing equations are $Re = 1142.8$, $Pr = 0.7$ and $Sc = 1.0$ while $\gamma = 1.4$. The computational domain is given in Table 1, where the physical domain is measured in terms of the initial shear layer momentum thickness $\delta_\theta(0)$. Such large domains are required to allow evolution to the self-similar state. The initial momentum thickness Reynolds number is $Re_\theta = 40$ while the Reynolds number based on vorticity thickness has an initial value of $Re_\omega = 160$. The final Reynolds numbers are large enough for turbulent flow, reaching values as large as 12,000. The integral length scales are sufficiently small compared to the dimensions of the computational box to have good large-scale resolution and the grid size is sufficiently small to resolve the small scales.

3 Analysis of the Compressibility Effect of Reduced Growth Rate

Figure 1 shows that the growth rate decreases with increasing M_c in the DNS, in close agreement with the Langley curve. Sarkar (1995), based on uniformly sheared flow DNS, suggested that decreased production is responsible for the reduction, with increasing Mach number, of the vorticity thickness growth rate and turbulent kinetic energy of the shear layer. In the case of the momentum thickness of the mixing layer, the compressibility effect of decreased growth rate must be associated with reduced level of normalized, integrated turbulent production according to Vreman *et al.* (1996). The current

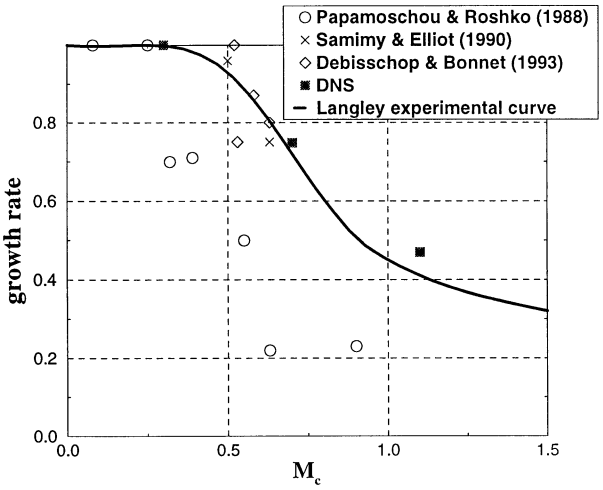

Figure 1. Dependence of the growth rate on M_c.

DNS also finds that the production, P, decreases with M_c. The Reynolds stress transport equations provide a simple yet effective method to further analyze the effect of compressibility and is considered below to answer the question as to why the Reynolds shear stress and, thereby, the turbulent production is inhibited in high-speed, compressible flow.

3.1 The Reynolds Stress Balance at High Speeds

The normalized transport equation for R_{11} is analyzed and after integrating across the self-similar coordinate, and introducing the overbar to denote the density-weighted integrals, the following equation for the growth rate, $\dot{\delta}_\theta$, is obtained:

$$\dot{\delta}_\theta \approx (\bar{\varepsilon}_{11} - \bar{\Pi}_{11}) \tag{1}$$

where $\bar{\varepsilon}_{11} = \int_{-\infty}^{\infty}(\bar{\rho}/\rho_o)(\varepsilon_{11}/\Delta u^3)dx_2$ and $\bar{\Pi}_{11} = \int_{-\infty}^{\infty}(\Pi_{11}/\rho_o \Delta u^3)dx_2$. From the DNS results, it is observed that the convective Mach number, M_c, affects $\bar{\varepsilon}_{11} - \bar{\Pi}_{11}$ by reducing its magnitude (notice that $\bar{\Pi}_{11}$ is negative) and, subsequently, the momentum thickness growth rate is reduced. Only $\bar{\Pi}_{11}$ is strongly affected by M_c, suggesting that the effect of M_c on the pressure-strain term is responsible for the reduction of the shear layer growth rate. The pressure strain term can only be reduced if the intensities of p' or $\partial u_1''/\partial x_1$ are reduced. From the DNS it is clear that the dominant reduction is in the rms pressure.

After confirming that the compressibility effects of reduced thickness growth rate and turbulence intensities are related to decreased pressure fluctuations, we now propose a mechanism for the altered pressure field.

3.2 The Pressure-Strain Term at High Speeds

In strictly incompressible flow, the instantaneous pressure has 'infinite' signal speed and satisfies a Poisson equation whose source is related to the velocity gradients. In the case of compressible flow, pressure fluctuations travel with the speed of sound, c_0. The consequence of a 'finite' signal speed on the pressure-strain term is now studied analytically.

The following evolution equation for p',

$$\frac{1}{c_o^2}\frac{D^2p'}{Dt^2} - \frac{\partial^2 p'}{\partial x_i \partial x_i} = \frac{\partial}{\partial x_i \partial x_j}\left(\rho u_i u_j\right)' \tag{2}$$

can be derived by taking the divergence of the momentum equation, and assuming that the isentropic relationship, $Dp/Dt = c_o^2 D\rho/Dt$, applies and viscous terms are negligible. Such assumptions are reasonable for high-Reynolds number flows away from shocks and solid boundaries. Eq. (2) is now specialized to the center of the shear layer where the mean velocity is zero, $\partial\tilde{u}_1/\partial x_2 \simeq$ constant, and an analysis, assuming locally-homogeneous turbulence, is performed. The result, for low Mach number, is

$$\frac{\Pi_{ij}}{\Pi_{ij}^I} = 1 - K_0 M_c^2 \tag{3}$$

which shows that Π_{ij} decreases with M_c as in the DNS.

The wave equation, Eq. (2), for the pressure is a useful approximation for analysis and is consistent with the energy equation, if the heat conduction and viscous dissipation terms are assumed negligible and the isentropic relation is assumed. These assumptions, although useful, are not physically supported for $M_c >> 1$. Therefore, at high Mach number, the general thermodynamic relation must be used,

$$\frac{Dp}{Dt} = \left(\frac{dp}{d\rho}\right)_s \frac{D\rho}{Dt} + \left(\frac{dp}{ds}\right)_\rho \frac{Ds}{Dt} \tag{4}$$

where the first term on the rhs is the 'acoustic' contribution and the second term is the 'entropy' contribution. Indeed, by taking the time derivative of Eq. (4) and using the divergence of the momentum equation, a modified wave equation for the pressure fluctuation results which involves entropy fluctuations and is valid for all Mach numbers. Analysis of the modified wave equation shows that $\Pi_{ij} \rightarrow const$, for large M_c. Thus, analysis provides functional forms for small and large Mach numbers.

A quantitative expression for the pressure-strain correlation which has the analytically predicted behavior at low and high Mach number is,

$$\frac{\Pi_{ij}}{\Pi_{ij}^I} = (1-c)\frac{1 + aM_c^2 e^{-(2M_c - 1/2)^2}}{1 + bM_c^2} + c \tag{5}$$

M_c	b_{11}	b_{22}	b_{12}
0.3	0.21	-0.08	0.18
0.7	0.37	-0.20	0.18
1.1	0.44	-0.25	0.17

Table 2. Peak values of the Reynolds stress anisotropy during its early-time evolution.

M_c	b_{11}	b_{22}	b_{12}
0.3	0.08	-0.06	0.15
0.7	0.10	-0.08	0.15
1.1	0.11	-0.09	0.15

Table 3. Long-time values of the Reynolds stress anisotropy.

where Π_{ij}^I is the predicted incompressible pressure-strain and the constants, $a = 4.0$, $b = 4.1$ and $c = 0.091$ were obtained by fitting to the 'experimental' values the asymptotic solutions, and using an exponential to approximate the difference at intermediate Mach numbers.

4 Anisotropy of the Reynolds Stress

The Reynolds stress anisotropy is an important characteristic of the velocity fluctuations that is used in advanced modeling of turbulent flows. Two important conclusions are drawn from the DNS. First, during its *initial* evolution, the anisotropy tensor is strongly affected by M_c, whereby larger magnitudes of the diagonal components of b_{ij} are measured for increasing M_c. Table 2 illustrates this trend using the peak anisotropies during the early-time transient. Second, after sufficiently long time, the values of the anisotropy tensor approaches asymptotic values that are only weakly dependent on M_c. Table 3 shows values from the self-similar region, where a weak increase of the normal stress anisotropies with M_c is observed while the off-diagonal component b_{12} remains constant. The peak values of turbulence intensities and shear stress at the center of the shear layer can also be considered and are preferable in comparing with experimental data. Comparisons with experimental results obtained by Samimy & Elliot (1990) and Barre *et al.* (1994) are in good agreement with the DNS.

5 Density Effect on the Growth Rate

The aim of series B is the study of the effect of density ratio on the growth rate. In this series, two parameters have been kept constant, the convective Mach number, M_c, and the average density, $\rho_o = (\rho_1 + \rho_2)/2$. Results corresponding to $s = 4$ and 8 are shown. Note that $s > 1$ implies that the upper stream has the lower density. Simulations with the reciprocal density ratios, $s = 1/4, 1/8$, were also performed but no difference was observed with respect to the $s = 4, 8$ cases regarding the growth rate. The influence of the density ratio on temporal growth rates of the vorticity thickness and the momentum thickness are investigated.

s	C_δ
1	0.117
4	0.137
8	0.125

Table 4. C_δ dependence on s for $M_c = 0.7$.

From similarity arguments, Brown (1974) derived an expression for the vorticity thickness growth rate dependence on the velocity and density ratios. The growth rate in a frame moving with the convection velocity, U_c, is defined by

$$\frac{1}{\Delta u}\frac{d\delta_\omega}{dt} = \dot{\delta}_\omega = \frac{C_\delta}{2} \tag{6}$$

Brown (1974) states that, although C_δ can be assumed independent of s, based on limited data available for low-speed flow, the convection velocity, U_c, shifts to the velocity of the high-density stream. Therefore, the spatial growth rate is modified by unequal free-stream densities. Brown (1974) and later Dimotakis (1984) proposed an expression that matched experimental data. Since the current DNS corresponds to a temporally evolving flow in a reference frame mandated to move with the convection velocity U_c, conclusions can be drawn with respect to the effect of s on solely C_δ and not U_c. Table 4 gives the values of C_δ for various density ratios and $M_c = 0.7$. It is clear that there is no appreciable dependence of C_δ on s in high-speed flow similar to the finding of Brown (1974) at low speeds.

Unlike the vorticity thickness, the growth rate of momentum thickness is found to decrease strongly with changes of density ratio from its reference value, $s = 1$. An analysis based on an expression which relates $\dot{\delta}_\theta$ to the product of mean density and Reynolds shear stress, $\bar{\rho}R_{12}$, integrated over the shear layer, is performed to understand the influence of s. DNS results show that the peak values of R_{12} do not change with s. However, there is a shift of the R_{12} profile towards the low-density stream. These observations together with the analysis predicts a density dependence of the form

$$\frac{\dot{\delta}_\theta}{\dot{\delta}_{\theta,1}} = 1 - 0.4\lambda(s)a(s) \tag{7}$$

where $\lambda(s) = (s-1)/(1+s)$, and $a(s)$, which is obtained from the DNS database, is a measure of the shift between density and velocity profiles. Table 5 shows that Eq. (7) agrees well with DNS results.

s	$\dot{\delta}_\theta/\dot{\delta}_{\theta,1}$	$1-0.4\lambda(s)a(s)$
1	1.00	1.00
4	0.86	0.82
8	0.59	0.70

Table 5. Density ratio effect on growth rate ratio.

6 Density Effect on Thermodynamic Statistics

Analysis of thermodynamic statistics reflect important changes due to the density differences. The case $M_c = 0.7$ is studied for density ratios of 1, 4 and 8. Consistent with the decrease of momentum thickness growth rate, there is a decrease of the pressure rms with increasing s. Nevertheless, the strongest effect of s is observed on the density and temperature fluctuations. Increases of up to one order of magnitude are observed for ρ_{rms} in Figure 2 as well as T_{rms} (not shown) with increasing values of s.

The temperature-density correlation, shown in Figure 3, shows a strong anti-correlation between fluctuations in T and ρ for the non-uniform density cases. Indeed, in the core of the shear layer, the correlation coefficient, $r_{T\rho} \to -1$, indicating dominance of the 'entropy' mode. The pressure-density correlation, not shown, changes strongly from the case $s = 1$ to the cases $s = 4, 8$. The strong near-unity correlation coefficient indicative of the 'acoustic' mode that is observed in the uniform density case progressively changes to lower values until negative values are achieved.

The turbulent Prandtl number, Pr_t, is obtained from the DNS data. There is little effect on the turbulent Prandtl number, with nominal values in the core of the shear layer ranging from 0.72 at $s = 1$, 0.81 at $s = 4$ and 0.9 at $s = 8$.

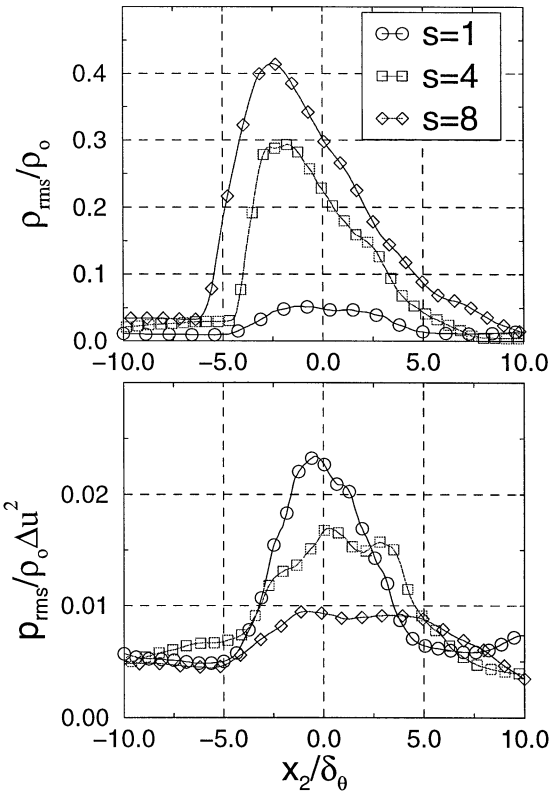

Figure 2. Density and Pressure fluctuations dependence on the density ratio, s.

7 Scalar Dissipation

The scalar dissipation, $\chi = \overline{\mu\nabla\zeta\cdot\nabla\zeta}/\bar{\rho}$, is the appropriate inverse 'fluid mechanical' time scale which should be compared with the chemistry time scales in order to determine the importance of finite-rate chemistry as discussed by Libby & Williams (1993). The normalized scalar dissipation is shown in Figure 4, where a relatively constant peak level of χ is observed, when scaled with the vorticity thickness and mean velocity difference. Similar to the effect on Reynolds stress profiles, the major effect of density ratio on scalar dissipation is the shift of peak χ to the low-density side.

8 Conclusions

The effect of the convective Mach number, M_c, as well as the density ratio, s, are studied for the turbulent shear layer. Large values of the Reynolds number are achieved which allows self-similar turbulence statistics. Based on analysis and DNS observations, a mechanism is proposed to explain the the important effect of compressibility that reduces the growth rate of the shear layer. This mechanism is directly related to the finite speed of sound, that leads to increased decorrelation

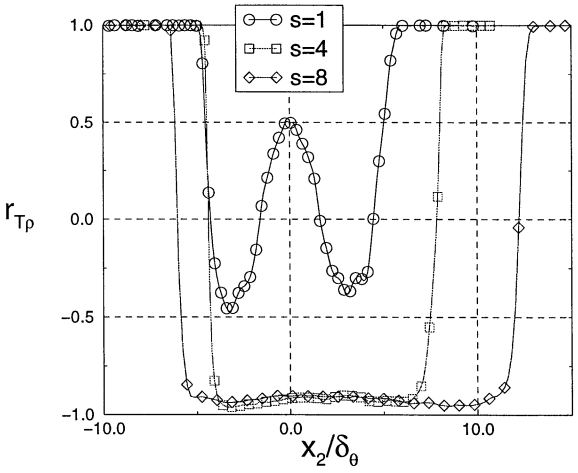

Figure 3. Density-Temperature Correlation.

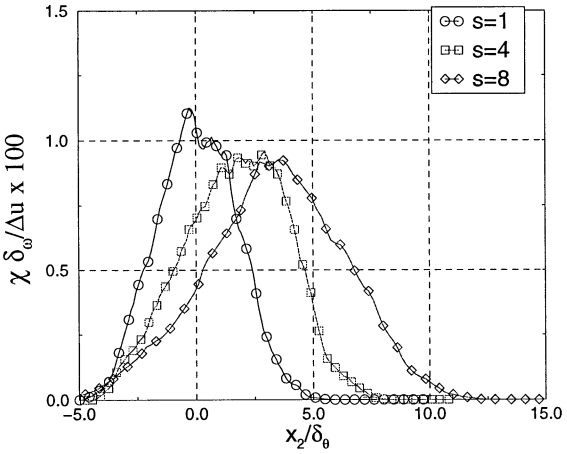

Figure 4. Normalized Scalar Dissipation.

in time between the pressure at adjacent points in the flow with increasing values of M_c. Consequently, the pressure-strain term, that provides the turbulence redistribution necessary to maintain shear-driven turbulence, decreases.

When the density ratio is varied for the $M_c = 0.7$ case, it is found that, although the vorticity thickness is insensitive to changes in s, the momentum thickness growth rate decreases. Interestingly, flipping the density ratio to $1/s$ from s has no influence on the growth rate of the temporal mixing layer. The maximum shear stress $\overline{uv}$ is found to remain invariant with s; however, its location shifts to the low-density side, thus, decreasing the momentum thickness growth rate.

When the density ratio increases, the density and temperature fluctuations are found to increase strongly while the pressure fluctuations decrease. The 'entropy' mode is found to dominate the 'acoustic' mode in the case of nonuniform density. The peak scalar dissipation rate, when normalized by the velocity difference and vorticity thickness, is found to be relatively insensitive to density ratio.

Acknowledgement

This work was supported by AFOSR through grant F49620-96-1-0106. Computational time was provided by the CEWES and NAVO Major Shared Resource Centers.

REFERENCES

BARRE, S., QUINE, C. & DUSSUAGE, J. 1994 Compressibility effects on the structure of supersonic mixing layers: experimental results. *J. Fluid Mech.* **259**, 47–78.

BOGDANOFF, D. 1983 Compressibility effects in turbulent shear layers. *AIAA J.* **21**, 926–927.

BRADSHAW, P. 1977 Compressible turbulent shear layers. *Ann. Rev. Fluid Mech.* **21**, 926–927.

BROWN, G. 1974 The Entrainment and Large Structure in Turbulent Mixing Layers. *5th Australasian Conf. on Hydraulics and Fluid Mechanics* pp. 352–359.

DIMOTAKIS, P. 1984 Two-dimensional shear layer entrainment. *AIAA J.* **24** (11), 1791–1796.

FREUND, J., MOIN, P. & LELE, S. 1997 *Compressibility Effects in a Turbulent Annular Mixing Layer*. Stanford Report No. TF-72.

KLINE, S. J., CANTWELL, B. J. & LILLEY, G. M. 1982 *Proc. 1980-81-AFOSR-HTTM-Stanford Conf. on Complex Turbulent Flows*, , vol. 1. Stanford University Press.

LELE, S. 1992 Compact Finite Differences Schemes with Spectral-like Resolution. *J. Comput. Phys.* **103**, 16–42.

LELE, S. 1994 Compressibility effects on turbulence. *Ann. Rev. Fluid Mech.* **26**, 211–254.

LIBBY, P. A. & WILLIAMS, F. A. 1993 *Turbulent Reacting Flows*. Academic Press.

MILLER, R., MADNIA, C. & GIVI, P. 1994 Structure of a turbulent reacting mixing layer. *Combust. Sci. and Tech.* **99**, 1–36.

PAPAMOSCHOU, D. & ROSHKO, A. 1988 The compressible turbulent shear layer: an experimental study. *J. Fluid Mech.* **197**, 453–477.

SAMIMY, M. & ELLIOT, G. 1990 Effects of Compressibility on the Characteristics of Free Shear Layers. *AIAA J.* **28** (3), 439–445.

SARKAR, S. 1995 The stabilizing effect of compressibility in turbulent shear flow. *J. Fluid Mech.* **282**, 163–186.

SARKAR, S. 1996 On density and pressure fluctuations in uniformly sheared compressible flow . *Proceedings, IUTAM Symposium on Variable Density Low-Speed Flows, Marseille, July 1996* .

SMITS, A. & DUSSAUGE, J. P. 1996 *Turbulent shear layers in supersonic flows*. American Institute of Physics Press.

THOMPSON, K. W. 1987 Time Dependent Boundary Conditions for Hyperbolic Systems. *J. Comput. Phys.* **68**, 1–24.

VREMAN, A., SANDHAM, N. & LUO, K. 1996 Compressible mixing layer growth rate and turbulence characteristics. *J. Fluid Mech.* **320**, 235–258.

WILLIAMSON, J. 1980 Low-Storage Runge-Kutta Schemes. *J. Comput. Phys.* **35**, 48–56.

ZALESAK, S. 1979 Fully multidimensional flux-corrected transport algorithms for fluids. *J. Comput. Phys.* **31**, 335–362.